machines

Article

The Effect of Using Tools with Protective Coatings on Changes in Surface Geometric Texture in High-Performance Machining of Cast Iron

Piotr Stieler, Daniel Grochała * and Rafał Grzejda *

Faculty of Mechanical Engineering and Mechatronics, West Pomeranian University of Technology in Szczecin, 70-310 Szczecin, Poland; piotr.stieler@gmail.com
* Correspondence: daniel.grochala@zut.edu.pl (D.G.); rafal.grzejda@zut.edu.pl (R.G.)

Abstract

Cast iron is a material widely used in mechanical engineering, the automotive industry and large-scale structures. Interest in cast iron remains strong, despite the widespread drive to manufacture ever lighter, cheaper and more durable machine parts from light metal alloys or titanium. This is mainly due to the low cost of cast iron, its ease of recycling and its favourable mechanical properties, including its particular ability to dampen vibrations. There are numerous publications in the international literature on the principles for selecting machining parameters for high-performance machining of steel, light metal alloys and titanium. Research into modelling the effect of machining parameters on the surface roughness and wear of cutting tools when machining these materials is widely documented. However, there is considerably less literature available on the high-performance machining of cast irons. This is particularly true in the context of the use of tools with protective coatings. To fill this gap, a research project was undertaken, which identified the potential for using a single tool for high-performance machining of spheroidal cast iron. The machining process was investigated under industrial conditions (in the automotive sector), taking into account the specific nature of roughing and finishing operations integrated into a single operation. In addition to investigating efficiency in terms of material removal and surface quality, the degree of wear on the cutting inserts at which the quality of the machined surface does not deteriorate was determined.

Keywords: protective coatings; surface geometric texture; high-performance machining; cast iron

Academic Editor: Kourosh Tatar

Received: 19 June 2026
Revised: 10 July 2026
Accepted: 15 July 2026
Published: 16 July 2026

1. Introduction

Modern technologies enable the manufacture of highly complex components with high dimensional and geometric accuracy. Alongside additive manufacturing techniques [1,2], which are growing in popularity, machining methods are constantly being developed [3,4]. It is thanks to these methods that it is possible to economically produce components of the highest precision, which meet stringent requirements regarding surface geometric texture (SGT) [5].

Continuous progress in the field of tool materials and computer numerical control (CNC) machine tools is opening up new prospects for subtractive manufacturing techniques. In modern industry, particular attention is paid to the development of machines, tools and software supporting the design of high-performance machining (HPM) technologies [6], implemented, amongst other things, on multi-axis machining centres.

 https://doi.org/10.3390/machines14070806

In large-scale and mass production, the key factor in process design is processing time, which is sometimes measured in seconds. To enable the production of hundreds or thousands of items within the limited time of a work shift, technological concentration is commonly employed. This primarily involves the use of special tools and fixtures based on automated clamping systems [7,8].

The potential of the entire manufacturing system is largely determined by the tools used. Careful selection of high-value cutting parameters can significantly reduce the machining time (i.e., the time taken to directly remove material) [9]. On the other hand, overly 'aggressive' parameters lead to accelerated wear of the cutting edges [10,11] and more frequent downtime associated with their replacement, which increases the proportion of auxiliary times. Production efficiency is therefore the result of machine availability, reduced by maintenance times and machining time, which is determined by technological parameters. For this reason, modern tool materials necessitate the design of solutions that enable operation at maximum cutting parameters whilst maintaining the longest possible tool life. Fallböhmer et al. [12] presented a method for optimising CNC programmes by adjusting the spindle speed and feed rate in order to maintain a near-constant chip load during the machining of cast iron workpiece surfaces.

When machining cast iron parts, including castings and forgings, short and brittle chips are produced [13]. This is due to the presence of hard matrix components and soft carbon inclusions in the form of graphite [14]. In industrial practice, it is common for tools designed for machining steel to be used for machining cast iron as well. However, it should be borne in mind that lower temperatures are generated when machining cast iron, which affects the wear mechanisms of the tool—the contact surface wears more rapidly. Importantly, tools designed exclusively for machining cast iron are not usually used for machining steel.

Cast iron castings and forgings are typically characterised by large machining allowances [15,16]. This is due to the solidification process, as a result of which the outer layer acquires a different structure to the inner layers. To achieve high dimensional and geometric accuracy, as well as the required surface finish, the machining process should be divided into roughing and finishing operations. This usually leads to a reduction in the degree of technological concentration due to the need for additional tool changes.

HPM of cast iron is a key process in the automotive, engineering and energy industries. As demands for surface quality, tool life and production efficiency increase, tools with protective coatings play an ever-greater role. These coatings are designed not only to increase wear resistance but also to influence the SGT of machined parts, which in turn affects the parts' performance characteristics [17,18]. These observations are accompanied by a growing demand for tools with extended service life and the ability to operate in extreme conditions, whilst maintaining a high-quality SGT [19,20].

The most used protective coatings in cast iron machining are nitrides and carbides of transition metals [21], as well as multilayer coatings, nanocomposites and functionally graded coatings [22,23]. The two main techniques for applying coatings to tools are chemical vapour deposition (CVD) and physical vapour deposition (PVD). CVD produces thick coatings with high adhesion and good wear resistance, but as they are applied at high temperatures, this can weaken the substrate [24]. PVD, on the other hand, provides thinner coatings that are better suited to sharp edges, but have lower adhesion. They are applied at lower temperatures [25]. The importance of the properties of tool coatings (CVD and PVD types) and the microstructure of compacted graphite cast iron for the selection of tools in extreme machining was presented by Esposito et al. [26]. They proposed taking into account, in a comprehensive manner, the properties of the tool, the properties of the workpiece, the cutting conditions and their mutual interaction, in order to assess the extent to which individual parameters influence machinability. Numerical simulations and experimental studies on the machining of compacted graphite cast iron using various coated tools at different stages of wear were carried out by Lai et al. [27]. The influence of microstructure, coating properties and tool wear on chip morphology, cutting force, temperature distribution and wear mechanisms was analysed. When machining cast iron under high loads or in dry conditions, it is possible to achieve higher productivity than that obtained with cemented carbide tools by using polycrystalline cubic boron nitride and ceramic tools [28,29].

Another way to improve the quality of SGT components made from cast iron and reduce tool wear is to use minimum quantity lubrication (MQL) [21] and hybrid cooling techniques [30]. Mardonov et al. [31] compared various lubrication strategies, including dry turning, flood cooling and MQL, in order to assess their effectiveness in reducing tool wear, lowering cutting temperatures and extending tool life. To investigate the influence of external lubrication and cooling conditions during the turning of AISI A48-25B grey cast iron, the mechanism of tool wear, the thermo-electromotive force generated in the cutting zone and flank wear were analysed. Uncoated WNMG 080408 cemented carbide inserts with a relief angle of 0° were used for the machining tests. Flank wear was halved in the MQL environment compared with dry and coolant-lubricant environments at high cutting speeds. To address the challenges associated with the use of conventional coolants, which have a negative economic and environmental impact, Peixoto et al. [32] developed a system of internally cooled tools for machining grey cast iron. In this system, the coolant circulates exclusively within the tool and the tool holder, thereby avoiding direct contact with the workpiece and the operator. Comparative analyses were carried out between system-based machining and dry machining, evaluating parameters such as surface roughness, cutting forces and tool wear mechanisms under various cutting conditions. The results showed that the developed system effectively reduced cutting forces and improved surface roughness compared with dry machining. Other aspects of using this system are summarised in [33].

Machining strategies for cast irons are closely linked to the sequence and nature of heat treatment. Machining prior to heat treatment ensures a longer tool life due to the lower hardness of the material but may require additional finishing operations after heat treatment. Partial (split) machining combines roughing machining before heat treatment with finishing after heat treatment, ensuring a balance between machinability and the part's structural properties. Machining after heat treatment is essential to achieve the final dimensions and surface finish, but increases tool wear due to the higher hardness and strain-induced transformations [34,35].

Statistical and computational methods, such as Taguchi methods and grey relational analysis, are widely used to optimise the many, often conflicting, objectives of machining cast iron (e.g., surface roughness, tool life, cutting efficiency) [36,37].

In summary, HPM of cast iron is a rapidly growing field, driven by advances in tooling, process optimisation and sustainable manufacturing. The ongoing implementation of intelligent control systems, advanced materials, the integration of heat treatment and machining to achieve optimum performance, and eco-friendly cooling strategies will be crucial for meeting future industrial and environmental demands requirements [38,39]. The development of tool materials, amongst other factors, played a key role in enabling HPM of cast irons [40,41]. Meanwhile, the available literature on HPM of cast iron remains limited. To expand knowledge in this area, a research project was carried out, as part of which the potential for using a single tool for HPM of spheroidal cast iron was identified. The machining process was evaluated under industrial conditions (in the automotive sector), with consideration given to the specific nature of roughing and finishing operations integrated into a single operation. Apart from assessing efficiency in terms of material

https://doi.org/10.3390/machines14070806

removal and surface quality, the degree of wear on the cutting inserts at which the quality of the machined surface does not deteriorate was established.

The research focused on the influence of machining parameters on tool life (taking into account three forms of wear) and the optimisation of cutting processes for parts manufactured in medium-sized series. In machine component manufacturing, these are non-standard production conditions for which there are no obvious solutions. Those designing manufacturing processes are often faced with the dilemma of whether to use dedicated (expensive) solutions or whether it is better to design the process based on universal solutions (which are not always cost-effective). The results of the research described in this paper may help to resolve this dilemma.

2. Materials and Methods

2.1. Research Object

The tests were carried out on castings made from EN-GJS-600-3U [42] spheroidal graphite cast iron—see Figure 1.

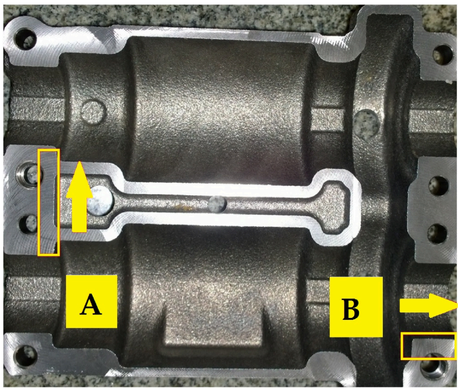

Figure 1. A view of the machined workpiece with sections A and B of the surface marked for SGT testing (the arrows indicate the direction of tool feed).

The spheroidisation process results in the formation of spherical graphite within the cast iron. Usually, the modification of the cast iron alloy involves adding spheroidising granules (magnesium or cerium) to the ladle prior to casting. This material must have a low sulphur and phosphorus content, and its matrix is usually ferrite, pearlite or a mixture of both. Thanks to the spherical structure of the graphite, ductile cast iron exhibits superior mechanical properties, including higher strength, ductility, impact resistance and hardness.

The standardised values for the mechanical properties of EN-GJS-600-3U cast iron for castings with wall thicknesses of up to 30 mm are shown in Table 1.

Table 1. Mechanical properties of EN-GJS-600-3U cast iron [43,44].

Tensile Strength, MPa	0.2% Proof Strength, MPa	Min. Elongation at Fracture, %	HBW Hardness
600	370	3	190 ÷ 270

EN-GJS-600-3U cast iron has a pearlitic-ferritic structure. In accordance with the foundry practices described in the relevant literature [45], the typical basic chemical composition required to achieve mechanical properties compliant with EN 1563 [44] for EN-GJS-600-3U cast iron falls within the ranges given in Table 2. In addition to the chemical elements listed in Table 2, magnesium and copper are also used in the production of EN-GJS-600-3U cast iron castings.

Table 2. Typical basic chemical composition of EN-GJS-600-3U cast iron [45].

Component	C	Si	Mn	P	S
Percentage composition	3.3 ÷ 3.8	2.15 ÷ 2.90	0.3 ÷ 0.8	up to 0.05	up to 0.01

2.2. Research Methodology

The tests were conducted using six-blade milling heads with a diameter of 50 mm, fitted with replaceable carbide inserts from Tungaloy (Tungaloy Corporation, Iwaki, Japan)—Figure 2a. The experiments were carried out under industrial conditions on a STAMA 334 TWIN twin-spindle milling centre (STAMA Maschinenfabrik GmbH, Schlierbach, Germany)—Figure 2b.

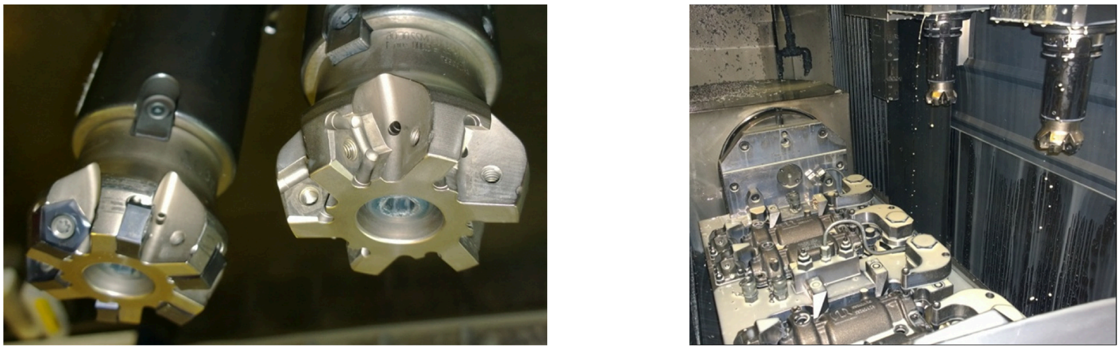

(**a**) (**b**)

Figure 2. Machining of the tested castings: (**a**) View of the tool heads; (**b**) View of workpieces clamped in the machine tool's work area.

Consistent machining conditions were maintained throughout the machining process. The machining of a single batch of cast semi-finished products was carried out by a single operator on the same machine tool, using a concentration of coolant-lubricant. During machining, flood cooling was used for both the tool and the workpiece. The cooling and lubricating fluid was prepared using demineralised water and the water-miscible metalworking fluid Rhenus TS 223 T [46] (Rhenus Lub GmbH & Co KG, Mönchengladbach, Germany).

The experimental plan involved testing the durability and cutting performance of two types of tool materials supplied by Tungaloy (Tungaloy Corporation, Iwaki, Japan). The first material was a general-purpose T1115 cemented carbide [47] (Figure 3—label T), which strikes a balance between the wear resistance of the cutting edge and the chipping that occurs on it. The second material was the AH120 cemented carbide [48] (Figure 3—label A), dedicated to machining cast iron.

For the general-purpose T1115 cemented carbide cutting inserts under investigation, Tungaloy (Tungaloy Corporation, Iwaki, Japan) applies multi-layer coatings (including TiN) using CVD technology. This process is supported by a special, proprietary (trade secret) surface treatment technology called PremiumTec, which smooths the surface and reduces residual stresses. The characteristics of this technology, which involves the high-temperature, layer-by-layer deposition of a CVD coating via a chemical reaction between gases, enable the production of a coating on T1115 carbide with a cellular layer structure, namely: a TiCN layer, an Al_2O_3 layer and an outer TiN layer (TiCN + Al_2O_3 + TiN). PremiumTec, on the other hand, involves smoothing the surface of the inserts, which prevents chip adhesion, reduces friction and improves resistance to chipping [49]. Meanwhile, what sets AH120 carbide inserts apart is not just the fine-grained sintered carbide, but its combination with the substrate and an advanced TiAlN PVD coating. The manufacturer also offers a special cutting edge preparation technology, PremiumTec, for this grade of insert. It is precisely this comprehensive combination of material and technology that enables AH120 inserts to meet the specific requirements associated with machining difficult-to-machine materials such as cast iron and stainless steels [50].

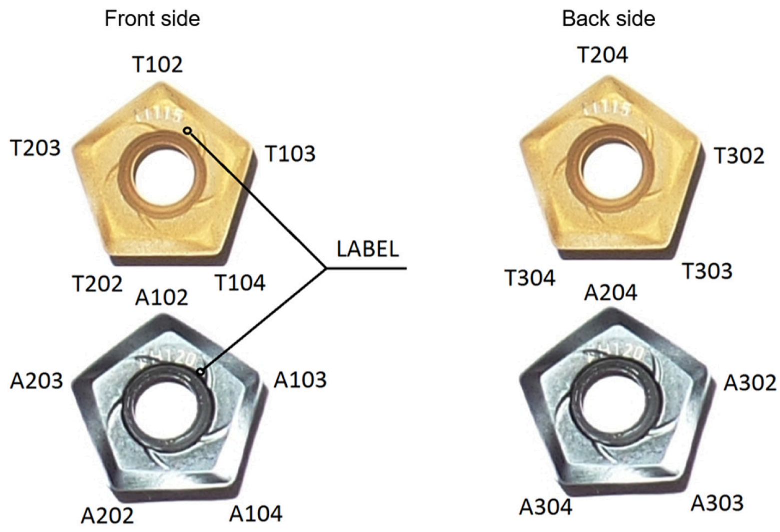

Figure 3. Identification of sides and edges on cutting inserts.

The comprehensive experimental plan for both carbide grades involved a total of 18 experiments. Each experiment was conducted using a new cutting edge by rotating the cutting inserts clockwise. Despite numerous changes to the positioning of the cutting inserts in the head, the same tightening torque of 3.0 Nm was applied to fixing screws each time using a torque wrench.

The designations of the individual cutting edges are shown in Figure 3. After completing five experiments on one side of the cutting insert, the insert was turned over to the other side.

Table 3 summarises the machining parameters selected for the insert tests. The machining parameters used were typical of rough milling, the aim of which is to achieve high volumetric productivity (at high cutting speeds v_c). When conducting the tests, the behaviour of the tools was also examined during finishing operations, in which minimising the feed rate per cutting edge f_z typically reduces geometric errors and the height-based roughness indices of the workpiece.

The range of variation in the technological cutting parameters was determined on the basis of the technical recommendations provided by the cutting insert manufacturer. The machine tool used was sufficiently rigid to ensure stable operating conditions throughout the test programme, and it was possible to eliminate any undesirable environmental influences.

The planned process specified a working stroke length for the tool (including approach and retract) along the cutting path (referred to as CD) of 0.65 m. Consequently, after machining 25 and 50 workpieces, the tool would have covered a cutting path of 16.25 m and 32.5 m, respectively. For each point in the experimental plan (from Table 3), a batch of 50 workpieces was produced. In total, 900 workpieces were processed during the experimental tests under industrial production conditions. The entire machining run of 900 workpieces was carried out without any downtime.

Measurements of SGT—in accordance with the technical documentation—were carried out on two sections of the surface (labelled A and B in Figure 1). In the sections designated for SGT measurement, there is a change in the cutting direction. It was expected that the highest surface irregularities would be found in these sections.

Table 3. Plan of tests on the durability of tools used for machining EN-GJS-600-3U cast iron, including the designation of individual configurations.

v_c, m/min	f_z, mm/Cutting Edge	T1115	AH120
100	0.2	T102	A102
	0.3	T103	A103
	0.4	T104	A104
200	0.2	T202	A202
	0.3	T203	A203
	0.4	T204	A204
300	0.2	T302	A302
	0.3	T303	A303
	0.4	T304	A304

The following three workpieces were selected for the SGT study: W1—the reference workpiece, W25—the central workpiece (from the middle of the respective series) and W50—the final workpiece. Measurements of SGT were conducted using a Hommel Etamic T1000 contact profilometer (Hommel Etamic, Villingen-Schwenningen, Germany) fitted with a Wave 20 self-levelling head and a TKU300/600 inductive sensor [51]. In the profile analysis, an element length of λ_c = 2.5 mm and a measurement length of l_n = 12.5 mm were adopted, with a cut-off value of 2.5 mm. As the tests were carried out under industrial conditions, the basic *Rz* index [52,53] was used to assess the roughness of the profiles under investigation. The tests were conducted in accordance with standard EN ISO 4288 [54], for which the maximum defined value of the *Rz* index was 12.0 µm. The *Rz* roughness index used served merely as an additional criterion for limiting the range of acceptable machining parameters (it was not a criterion for process optimisation).

The measurement results and assessment of the product surfaces were based on the 16% rule [55]. In most cases, a single measurement was taken per test section. A greater number of measurements were taken in test sections where the permissible value of the *Rz* index was exceeded or where the measured *Rz* value was ≥11.0 µm. In such cases, an average value was determined based on 3 or 5 surface profile measurements, respectively.

In the wear tests on multi-edged cutting inserts, geometric wear indices were also determined (Figure 4a), such as wear width at the contact surface *VB*, wear width at the contact surface at the corner of the cutting edge *VBc* and cutting edge corner retraction *KE*. These values were determined using a Hawk Duo measuring microscope (Vision Engineering Ltd., Send, UK) [56]. The device was equipped with a video camera connected to a 10× optical lens and M-Series metrology software. The geometric wear indices were established using the symmetry of the cutting edge. First, the centre of the cutting edge was identified, and then the distance between it and the section of the edge that did not participate in the cutting process was measured (Figure 4b).

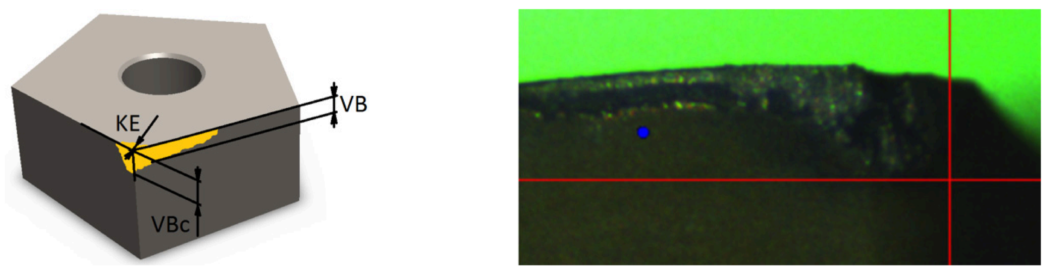

(**a**) (**b**)

Figure 4. Wear tests on cutting inserts: (**a**) Determining geometric wear indices; (**b**) wear width at the contact surface in the corner *VBc* = 0.444 mm for point T304 in the experimental plan. (The maximum permissible wear on the cutting edge *VBm* was set at 0.3 mm, in accordance with [57]).

3. Results

The results of surface roughness measurements following the machining of workpieces W1, W25 and W50 are collected in Table 4.

Table 4. Surface roughness measured after machining workpieces W1, W25 and W50 using defined configurations.

Workpiece	Section	*Rz*, µm																	
		T102	**T103**	**T104**	**T202**	**T203**	**T204**	**T302**	**T303**	**T304**	**A102**	**A103**	**A104**	**A202**	**A203**	**A204**	**A302**	**A303**	**A304**
W1	A	5.95	9.78	8.50	4.58	5.63	10.5	6.61	4.47	6.48	5.76	5.60	6.10	4.66	8.41	7.31	3.70	4.69	7.95
	B	5.79	7.50	7.56	2.70	4.80	6.11	3.77	3.79	4.79	5.62	5.83	5.89	3.51	5.69	6.51	3.45	4.14	4.96
W25	A	6.90	10.7	6.52	9.20	12. 9	13.8	6.65	5.55	8.41	8.91	10.2	7.44	8.87	11.1	8.71	6.26	7.17	8.01
	B	6.36	11.2	7.89	6.00	5.97	9.84	4.38	3.76	5.04	8.38	9.64	9.77	5.83	7.57	6.68	4.56	4.44	6.93
W50	A	7.09	11.7	13.0	11.5	14.0	14.2	14.0	9.10	9.25	10.5	9.66	11.2	10.2	13.4	8.67	8.79	7.72	9.74
	B	8.22	9.39	9.13	5.92	9.11	10.9	8.03	4.66	6.67	9.13	9.17	10.5	6.87	7.86	8.24	3.78	4.84	7.15

The results of the roughness measurements are also presented in bar charts, with a constant scale for the *Rz* index, in Figures 5–7. The relevant CD values have also been added to the charts.

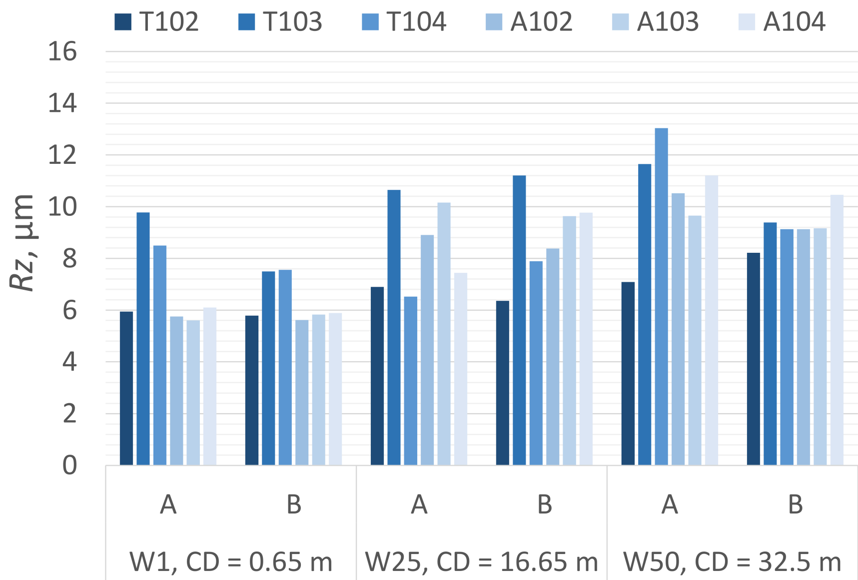

Figure 5. *Rz* roughness in the surface profile obtained after machining successive workpieces at a speed of v_c = 100 m/min.

The values obtained for the wear indices of the inserts on the contact surface and the blade corner reduction are listed in Table 5. The results of these measurements are also shown graphically in Figure 8.

Table 5. Wear index values for the individual configurations in the test plan.

i [1]	T102	T103	T104	T202	T203	T204	T302	T303	T304	A102	A103	A104	A202	A203	A204	A302	A303	A304
VB, mm	0.173	0.147	0.162	0.135	0.173	0.212	0.220	0.185	0.172	0.114	0.125	0.126	0.094	0.105	0.143	0.103	0.134	0.129
VB_C, mm	0.065	0.000	0.110	0.248	0.000	0.174	0.586	0.488	0.444	0.000	0.000	0.000	0.045	0.090	0.000	0.290	0.000	0.000
KE, mm	0.008	0.008	0.000	0.047	0.006	0.019	0.029	0.054	0.079	0.030	0.037	0.032	0.016	0.041	0.038	0.025	0.038	0.034

[1] Designation of a given point in the experimental plan.

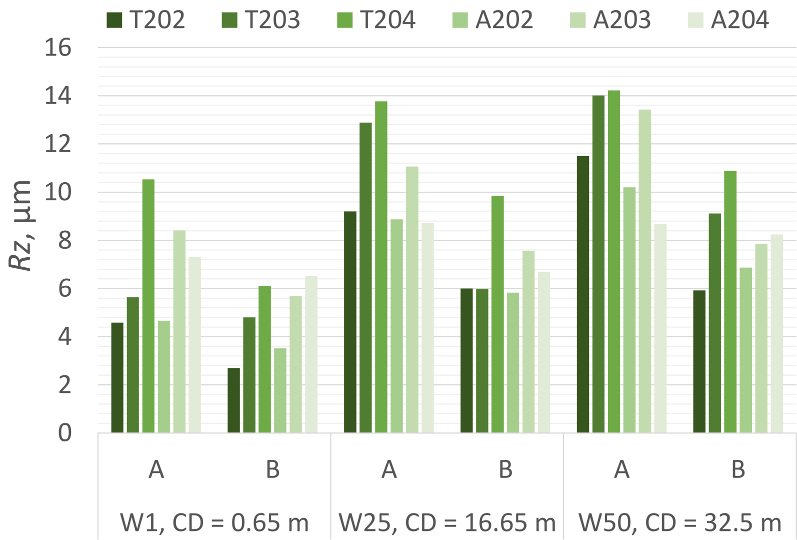

Figure 6. *Rz* roughness in the surface profile obtained after machining successive workpieces at a speed of v_c = 200 m/min.

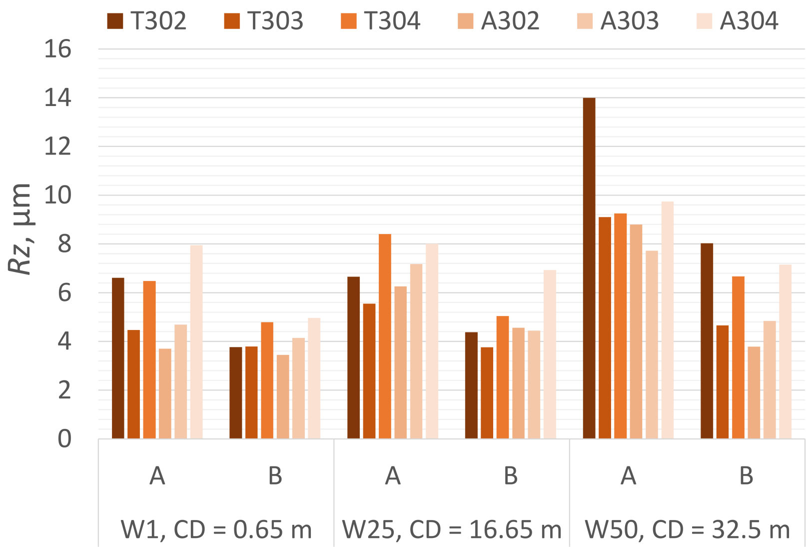

Figure 7. *Rz* roughness in the surface profile obtained after machining successive workpieces at a speed of v_c = 300 m/min.

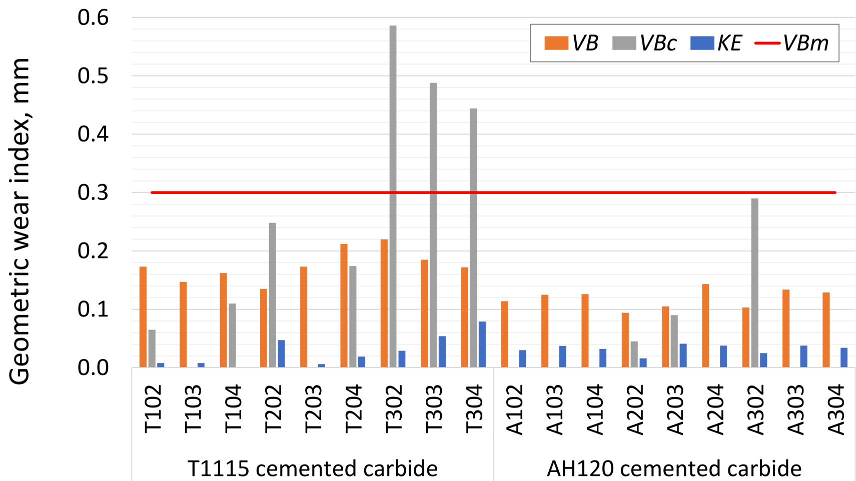

Figure 8. Geometric values of insert wear indices during the machining of EN-GJS-600-3U cast iron.

4. Discussion

4.1. Assessment of the Roughness of Machined Surfaces

The highest average roughness values were obtained when machining the cast iron under test at a speed of v_c = 100 m/min. The difference between the *Rz* roughness index values for the reference workpiece and the final workpiece in the series was just under 30% when machining with T-type inserts and just under 73% when machining with A-type inserts (Figure 5). When machining the reference workpiece with a cutting insert designed for machining cast iron (i.e., AH120), the surface roughness of the profiles was approx. 23% lower. The inserts, made from the versatile T1115 carbide grade, ran in quite effectively after machining the first workpiece. This resulted in a lower surface roughness on the workpieces. Towards the end of the series, an increase in the *Rz* roughness index was observed, caused by gradually increasing wear. This effect was also observed for inserts made from AH120 carbide, although to a much lesser extent. Inserts designed for machining cast iron produced an average *Rz* roughness index value that was approx. 3% lower. Unfortunately, for the T1115 carbide, the *Rz* tolerance limit was found to have been exceeded following the machining of the last workpiece (for f_z = 0.4 mm/cutting edge).

When machining at a speed of v_c = 200 m/min, the T1115 versatile cemented carbide produced a lower average surface roughness on the first workpiece. However, as machining of subsequent workpieces progressed, the surface roughness increased very rapidly—Figure 6. In contrast, the AH120 cemented carbide, designed specifically for machining cast iron, enabled a more consistent and predictable surface roughness to be achieved when cutting at a speed of v_c = 200 m/min. Despite the reference workpiece initially having higher roughness values, a slight increase in the *Rz* value was observed in this case as the surfaces of subsequent workpieces were machined. A smaller variation in the *Rz* roughness values is clearly noticeable for inserts designed for machining cast iron. In this point of the experimental plan, the AH120 material enabled an average *Rz* roughness value that was nearly 13% lower and a roughness level that was almost 16% lower after machining 50 workpieces. Higher cutting speed contributes to a more rapid increase in roughness values, which is particularly dangerous for T1115 material, where the permissible value for the *Rz* roughness index was exceeded after machining just 25 workpieces. In one of the experiments carried out, the permissible value for the *Rz* roughness index was also found to have been exceeded when using a cutting insert made from the dedicated AH120 material (for f_z = 0.3 mm/cutting edge).

For both types of carbide, favourable results were observed when machining cast iron at a speed of v_c = 300 m/min. At all points in the experimental plan, the lowest values of the surface roughness index *Rz* were obtained. This highly favourable situation makes it possible to achieve the required SGT as early as the roughing and shaping operations—Figure 7. Although an increase in the roughness values of the finished workpiece compared with the initial workpiece was observed, for pre-run-in cutting edges the increase in surface roughness proceeds at a much slower rate. The observed increase in the *Rz* surface roughness index value for the centre workpiece was 13% and 29% for machining with carbide tools T1115 and AH120, respectively. By contrast, the further increase in the *Rz* value for the final workpiece was 53% and 12% for machining with carbide T1115 and AH120, respectively. Inserts designed for machining cast iron yielded an average roughness value that was approx. 6% lower in this point of the experimental plan.

Taking into account all the test results (Figures 5–7), the use of AH120 cemented carbide, which is specifically designed for machining cast iron, is very safe at high cutting speeds and feed rates.

https://doi.org/10.3390/machines14070806

4.2. Assessment of the Degree of Insert Wear

During the tests at a speed of v_c = 100 m/min, the greatest wear width at the contact surface *VB* was observed for T1115 cemented carbide cutting inserts and varied between 0.147 mm and 0.173 mm—Figure 8. The cutting edges of the inserts made from AH120 carbide were characterised by a lower *VB* index value, which varied between 0.114 mm and 0.126 mm. For inserts made of AH120 material and at a cutting speed of v_c = 100 m/min, no wear occurred on the contact surface at the corner of the cutting edge (*VBc* was equal to 0 in every case). Meanwhile, for T1115 carbide cutting inserts, the wear on the contact surface at the corner of the cutting edge was 0.065 mm at a feed rate of f_z = 0.2 mm/cutting edge, and 0.11 mm at a feed rate of f_z = 0.4 mm/cutting edge. On each attempt, the cutting edge corner retraction *KE* was between 0.03 and 0.04 mm. Interestingly, the cutting edge of inserts made from the universal carbide grade T1115 showed virtually no reduction in length. The *KE* values obtained in this case, with a maximum of 0.008 mm, fall within the measurement uncertainty range of the microscope used.

At a cutting speed of v_c = 200 m/min for both materials (T1115 and AH120), the wear width at the contact surface *VB* increased as the feed rate per cutting edge increased. Significantly higher *VB* values were recorded for inserts made from T1115. The highest value of wear on the contact surface at the corner of the cutting edge made from T1115 material, *VBc* = 0.248 mm, was recorded at a feed rate of f_z = 0.2 mm/cutting edge. The maximum value of this parameter for inserts made of AH120 material (*VBc* = 0.09 mm) took place at a feed rate of f_z = 0.3 mm/cutting edge. In all the cases considered, the cutting edge was shortened. The greatest retraction in cutting edge length for inserts made of AH120 material was observed at a feed rate of f_z = 0.3 mm/cutting edge (*KE* = 0.041 mm). In contrast, the wear value of *KE* = 0.047 mm was highest for T1115 cutting inserts at a feed rate of f_z = 0.2 mm/cutting edge.

The value of wear width at the contact surface *VB* at a cutting speed of v_c = 300 m/min was significantly lower for inserts made of AH120 material and did not exceed 0.14 mm. For cutting inserts made of T1111 carbide, the minimum *VB* value of 0.172 mm was reached at a feed rate of f_z = 0.4 mm/cutting edge. Conversely, the maximum *VB* value of 0.22 mm was reached at a feed rate of f_z = 0.2 mm/cutting edge. By far the greatest wear occurred on the contact surface at the corner of the cutting edge was recorded at a cutting speed of v_c = 300 m/min for inserts made from T1115 carbide. The maximum value of *VBc* = 0.586 mm occurred at a feed rate of f_z = 0.2 mm/cutting edge and decreased as the feed rate increased. A high value of *VBc* = 0.29 mm was also noted for inserts made from AH120 carbide, which is specifically designed for machining cast iron, at a feed rate of f_z = 0.2 mm/cutting edge. The retraction in cutting edge length *KE* for the AH120 material did not exceed 0.04 mm, whereas for the T1115 material, the *KE* value increased in line with the feed rate on the cutting edge, ranging from 0.029 to 0.079 mm.

4.3. Development of Research Findings

The average roughness value determined from the measurement of the final workpiece $\overline{Rz}_{(W50)}$ on sections A and B was adopted as the technological index for analysing the degree of wear, in accordance with the following equation:

$$\overline{Rz}_{(W50)} = \frac{Rz_{(W50;\ A)} + Rz_{(W50;\ B)}}{2} \quad (1)$$

where $\overline{Rz}_{(W50;\ A)}$—average roughness determined for section A; $\overline{Rz}_{(W50;\ B)}$—average roughness determined for section B.

The average roughness values $\overline{Rz}_{(W50)}$ obtained were then normalised within the range $\langle 0,\ 1\rangle$ [58] using the following formula:

$$Norm_{(Rz)i} = \frac{\overline{Rz}_{(W50)i} - \overline{Rz}_{(W50)min}}{\overline{Rz}_{(W50)max} - \overline{Rz}_{(W50)min}} \tag{2}$$

where $\overline{Rz}_{(W50)i}$—average roughness value for *i*-th point in the experimental plan (see Table 5); $\overline{Rz}_{(W50)min}$—minimum average value of the roughness index (see Table 6); $\overline{Rz}_{(W50)max}$—maximum average value of the roughness index (see Table 6).

Table 6. Summary of the standardised values obtained for surface roughness and insert wear indices.

i	$\overline{Rz}_{(W50)i}$	$Norm_{(Rz)i}$	$Norm_{(VB)i}$	$Norm_{(VBc)i}$	$Norm_{(KE)i}$	$NSUM_i$
T102	7.66	0.22	0.63	0.11	0.10	1.06
T103	10.5	0.68	0.42	0.00	0.10	1.20
T104	11.1	0.77	0.54	0.19	0.00	1.49
T202	8.71	0.39	0.33	0.42	0.59	1.73
T203	11.6	0.84	0.63	0.00	0.08	1.55
T204	12.6	1.00	0.94	0.30	0.24	2.47
T302	11.0	0.75	1.00	1.00	0.37	3.12
T303	6.88	0.10	0.72	0.83	0.68	2.33
T304	7.96	0.27	0.62	0.76	1.00	2.64
A102	9.83	0.56	0.16	0.00	0.38	1.10
A103	9.42	0.50	0.25	0.00	0.47	1.21
A104	10.8	0.73	0.25	0.00	0.41	1.38
A202	8.54	0.36	0.00	0.08	0.20	0.64
A203	10.7	0.70	0.09	0.15	0.52	1.46
A204	8.46	0.35	0.39	0.00	0.48	1.22
A302	6.29	0.00	0.07	0.49	0.32	0.88
A303	6.28	0.00	0.32	0.00	0.48	0.80
A304	8.45	0.35	0.28	0.00	0.43	1.05

On the basis of relationships analogous to Equation (2), the values of the geometric values of insert wear indices were also normalised. This yielded: the normalised wear width at the contact surface $Norm_{(VB)i}$, the normalised wear width at the contact surface at the corner of the cutting edge $Norm_{(VBc)i}$ and the normalised cutting edge corner retraction $Norm_{(KE)i}$—see Table 6.

Finally, the sum of the normalised values was calculated as follows:

$$NSUM_i = Norm_{(Rz)i} + Norm_{(VB)i} + Norm_{(VBc)i} + Norm_{(KE)i} \tag{3}$$

It was assumed that a situation in which the permissible value of the *Rz* roughness index was exceeded, caused by the maximum observed forms of cutting insert wear, would result in a normalised sum of $NSUM_i = 4$. Such a situation would have to be regarded as the worst-case technological scenario for machining EN-GJS-600-3U cast iron.

The lowest $NSUM_i$ value makes it easy to identify the most favourable machining scenario (i.e., the one resulting in the lowest surface roughness and the least wear on the cutting insert). Furthermore, by visualising the results in a table using a 'heat map' [59], the effectiveness of both cermet grades under investigation can be efficiently compared.

Based on the data in Table 6, it can be concluded that the most favourable of the cast iron machining cases studied is the A202 configuration. It involved machining cast iron using a dedicated insert made of AH120 material at a speed of v_c = 200 m/min and a feed rate of f_z = 0.2 mm/cutting edge. Although this configuration does not specify a minimum value for the *Rz* roughness index, the observed minimal tool wear suggests that it will offer the longest tool life (for comparison, see [60]). Milling in this way allows the lowest tooling costs to be achieved.

However, one of the most cost-effective methods for machining short production runs is to combine a cutting speed of v_c = 300 m/min with a feed rate of f_z = 0.3 mm/cutting edge (A303 configuration). This configuration has also yielded some of the lowest *Rz* roughness index values recorded. It should be borne in mind that, thanks to its superior surface finish and greater dimensional accuracy, EN-GJS-600-3U cast iron is suitable for applications requiring high performance (e.g., in the automotive and energy sectors) [61].

AH120, a cermet specifically designed for machining cast iron, delivers good performance across the entire range of machining parameters tested, particularly at higher cutting speeds and feeds. On an ad hoc basis, cutting inserts made from the universal T1115 cemented carbide grade may be used for machining cast iron. However, in this case, minimising surface roughness and extending tool life results in low economic efficiency of the process (T102 configuration), where a cutting speed of v_c = 100 m/min with a feed rate of f_z = 0.2 mm/cutting edge is permissible.

According to the experimental results obtained, the cutting speed v_c had a greater influence on changes in the *Rz* index than changes in the feed rate f_z (regardless of the type of cemented carbide used). This phenomenon can be explained by the fact that EN-GJS-600-3U cast iron contains graphite spheres, which cause brittle fracture of the material during machining. At lower speeds, material particles are more frequently torn out, and micro-spalling occurs on the surface. Within the range of cutting parameters under investigation, there is a change in the dominant mechanism responsible for surface formation (i.e., changes in the *Rz* index value). At low speeds, high *Rz* values are observed, typical of spalling and the ejection of material particles from surfaces machined at excessively low speeds. The mechanism of stable kinematic and geometric reproduction of the tool edge began to dominate at cutting speeds of v_c = 200 m/min and above. In turn, a change in feed rate f_z within the range of 0.1–0.3 mm/cutting edge mainly affected the geometric component of surface roughness. Under the conditions analysed, due to the large corner radius of the cutting insert, this had less significance than material and dynamic phenomena.

In none of the experiments carried out did the cutting insert reach the permissible surface wear value *VBm*. Using the linear relationship, the expected number of workpieces, $\hat{W}_{(0.3)}$, was estimated as follows:

$$\hat{W}_{(0.3)} = \frac{50 \cdot VBm}{VB_i} \quad (4)$$

where *VBm*—maximum permissible wear on the cutting edge (equal to 0.3 mm—see Figures 4 and 8); VB_i—wear value measured on the surface of the insert after producing 50 workpieces.

The values for the number of workpieces that can be machined using the recommended machining parameters are shown in Table 7.

Throughout the experiment, inserts made from AH120 cemented carbide demonstrated a higher average value of abrasive wear resistance (*VB*) than those made from T1115 when machining EN-GJS-600-3U cast iron, by approximately 32%. This allowed an estimate to be made that, on average, up to 46% more workpieces can be machined using these inserts.

Table 7. Expected numbers of workpieces produced using the proposed machining parameters.

i [1]	T102	T103	T104	T202	T203	T204	T302	T303	T304	A102	A103	A104	A202	A203	A204	A302	A303	A304
$\hat{W}_{(0.3)}$	87	102	93	111	87	71	68	81	87	132	120	119	160	143	105	146	112	116

[1] Designation of a given point in the experimental plan.

5. Conclusions

The research carried out made it possible to determine the wear of the inserts under specified cutting parameters and their impact on the surface quality of the workpiece. A carefully conducted series of experiments yielded reliable results, which provide valuable information on the machinability of EN-GJS-600-3U cast iron. The research enabled the selection, under industrial production conditions, of appropriate machining parameters to ensure continuous machining (corresponding to the A303 configuration). It was confirmed that the use of advanced tool materials and optimised parameters increases tool life and machining efficiency. This directly reduces the production costs of EN-GJS-600-3U castings [62].

On the basis of the measurements carried out and the analysis of the results obtained, the following specific conclusions can be drawn:

1. As machining progresses, the rate of change in surface roughness increases. This increase is initially significant, then stabilises, which is due to the natural running-in of the insert's cutting edge.
2. The lowest values of the *Rz* surface roughness coefficient were obtained at a cutting speed of v_c = 300 m/min for the AH120 carbide grade. In contrast, for the T1115 general-purpose carbide, one of the highest *Rz* roughness values was observed at this speed and a feed rate of f_z = 0.2 mm/cutting edge.
3. For the AH120 carbide grade, an increase in cutting speed results in lower surface roughness values, whereas for the T1115 carbide grade, the lowest surface roughness values are achieved at a cutting speed of v_c = 200 m/min.
4. The feed rate per cutting edge has less of an effect on surface roughness when machining with AH120 carbide inserts and at cutting speeds of 100–200 m/min. Cutting speed has a greater effect on surface roughness than the feed rate per cutting edge.
5. For the T1115 carbide grade, an increase in cutting speed leads to greater wear of the contact surface at the corner of the cutting edge *VBc*, whilst an increase in feed rate per cutting edge reduces this wear in the range v_c = 200–300 m/min.
6. In every case, the cutting edge corner retraction *KE* of the AH120 carbide grade was shortened. This is due to the cutting edge of the insert becoming worn in. For the T1115 carbide grade, the shortening of the *KE* led to significant wear of the contact surface at the corner of the cutting edge *VBc*. The protective coating was abraded, resulting in cutting edge loss across the full cutting depth.

Author Contributions: Conceptualisation, P.S. and D.G.; methodology, D.G.; software, P.S.; validation, D.G. and R.G.; formal analysis, D.G. and R.G.; investigation, P.S. and D.G.; resources, P.S.; data curation, P.S. and D.G.; writing—original draft preparation, D.G. and R.G.; writing—review and editing, R.G.; visualisation, D.G.; supervision, D.G.; project administration, R.G.; funding acquisition, R.G. All authors have read and agreed to the published version of the manuscript.

Funding: This research received no external funding.

Data Availability Statement: The original contributions presented in this study are included in the paper. Further inquiries can be directed to the corresponding authors.

Conflicts of Interest: The authors declare no conflicts of interest.

Abbreviations

The following abbreviations are used in this paper:

CD	Cutting distance
CNC	Computer numerical control

CVD	Chemical vapour deposition
HPM	High-performance machining
MQL	Minimum quantity lubrication
PVD	Physical vapour deposition
SGT	Surface geometric texture

References

1. Krawczyk, M.; Powalka, B.; Matuszak, M.; Fryska, S.; Grzesiak, D.; Figiel, P. The role of the additive manufacturing process parameters in the shaping of the surface geometric structure during micro-milling. *J. Mach. Eng.* **2020**, *20*, 86–93. [CrossRef]
2. Terelak-Tymczyna, A.; Bachtiak-Radka, E.; Grzesiak, D.; Jardzioch, A. Comparison of the classic and hybrid production methods with the use of SLM taking into account the aspects of sustainable production development. *Adv. Sci. Technol. Res. J.* **2023**, *17*, 94–107. [CrossRef]
3. Dudzinska, S.; Szydlowski, M.; Grochala, D.; Bachtiak-Radka, E. Application of correlation function for analysis of surface structure shaping by hybrid manufacturing technology. In *Advances in Manufacturing*; Hamrol, A., Ciszak, O., Legutko, S., Jurczyk, M., Eds.; Springer: Cham, Switzerland, 2018; pp. 651–659.
4. Grochała, D.; Grzejda, R.; Józwik, J.; Siemiątkowski, Z. Improving the degree of surface isotropy of parts manufactured using hybrid machining processes. *Coatings* **2025**, *15*, 461. [CrossRef]
5. Grzejda, R.; Grochała, D. The effect of normal load on the change in geometrical texture of surfaces forming a multi-bolted connection. *Appl. Sci.* **2026**, *16*, 3248. [CrossRef]
6. Chiron Group Technologies. Available online: https://chiron-group.com/technologies (accessed on 19 June 2026).
7. Kaliński, K.J.; Galewski, M.A.; Stawicka-Morawska, N.; Jemielniak, K.; Mazur, M.R. The clamping selection method to reduce the vibration of large-size workpieces during the face milling process. *Bull. Pol. Acad. Sci. Tech. Sci.* **2024**, *72*, e148840.
8. Kaliński, K.J.; Stawicka-Morawska, N.; Galewski, M.A.; Mazur, M.R. Mechatronic design techniques to predict the best clamping conditions in slender ball end milling of a flexible workpiece. *Adv. Sci. Technol. Res. J.* **2026**, *20*, 264–283. [CrossRef]
9. Burek, J.; Zylka, L.; Plodzien, M.; Gdula, M.; Sulkowicz, P. The influence of the cutting edge shape on high performance cutting. *Aircr. Eng. Aerosp. Technol. Int. J.* **2018**, *90*, 134–145. [CrossRef]
10. Twardowski, P.; Legutko, S.; Krolczyk, G.M.; Hloch, S. Investigation of wear and tool life of coated carbide and cubic boron nitride cutting tools in high speed milling. *Adv. Mech. Eng.* **2015**, *7*, 1687814015590216. [CrossRef]
11. Matuszak, J.; Zaleski, K.; Zyśko, A. Investigation of the impact of high-speed machining in the milling process of titanium alloy on tool wear, surface layer properties, and fatigue life of the machined object. *Materials* **2023**, *16*, 5361. [CrossRef] [PubMed]
12. Fallböhmer, P.; Rodríguez, C.A.; Özel, T.; Altan, T. High-speed machining of cast iron and alloy steels for die and mold manufacturing. *J. Mater. Process. Technol.* **2000**, *98*, 104–115. [CrossRef]
13. Li, S.; Lin, H.; Zhang, T.; Sui, J.; Wang, C. High-speed machining of malleable cast iron by various cutting tools coated by physical vapor deposition. *Chin. J. Mech. Eng.* **2021**, *34*, 46. [CrossRef]
14. Olawale, J.O.; Ibitoye, S.A.; Oluwasegun, K.M. Processing techniques and productions of ductile iron: A review. *Int. J. Sci. Eng. Res.* **2016**, *7*, 397–423.
15. Favi, C.; Campi, F.; Mandolini, M.; Martinelli, I.; Germani, M. Key features and novel trends for developing cost engineering methods for forged components: A systematic literature review. *Int. J. Adv. Manuf. Technol.* **2021**, *117*, 2601–2625. [CrossRef]
16. Miyamoto, Y.; Shiraoka, S.; Kuramoto, Y.; Ri, B. Production of Heavy-Section 6-Ton High-strength Ductile Iron Castings for Steam-Tube Dryer Roller. *Int. J. Met.* 2026, *in press*. [CrossRef]
17. Fiorini, P.; Byrne, G. The influence of built-up layer formation on cutting performance of GG25 grey cast iron. *CIRP Ann. Manuf. Technol.* **2016**, *65*, 93–96. [CrossRef]
18. de Sousa, J.A.G.; Sales, W.F.; Machado, A.R. A review on the machining of cast irons. *Int. J. Adv. Manuf. Technol.* **2018**, *94*, 4073–4092.
19. Zheng, L.J.; Lai, Z.W.; Sun, Y.; Chen, L.; Wang, J.; Jawahir, I.S.; Wang, C.Y. The machining of compacted graphite irons—State of the art and future perspective. *Mach. Sci. Technol.* **2025**, *29*, 118–157. [CrossRef]
20. Laouissi, A.; Atmani, D.; Guendouz, H.; Safi, K.; Djermoune, A.; Yallese, M.A. Wear behavior of uncoated and coated Si_3N_4-based ceramic tool, and their effect on surface integrity in dry machining of gray cast iron. *Int. J. Refract. Met. Hard Mater.* **2026**, *135*, 107527. [CrossRef]
21. Zgrzeblak, S.; Grochała, D.; Grzejda, R. On the possibility of improving surface geometrical texture during high-performance machining of aluminium without the use of coolant. *Coatings* **2025**, *15*, 971. [CrossRef]
22. Derflinger, V.; Brändle, H.; Zimmermann, H. New hard/lubricant coating for dry machining. *Surf. Coat. Technol.* **1999**, *113*, 286–292. [CrossRef]
23. Perucca, M.; Durante, S.; Semmler, U.; Rüger, C.; Fuentes, G.G.; Almandoz, E. Cast iron cutting with nano TiN and multilayer TiN-CrN coated inserts. *IOP Conf. Ser. Mater. Sci. Eng.* **2012**, *40*, 012004. [CrossRef]

24. Fuentes, G.G.; Almandoz, E.; Rodríguez, R.J.; Dong, H.; Qin, Y.; Mato, S.; Pérez-Trujillo, F.J. Vapour deposition technologies for the fabrication of hot-forming tools: A review. *Manuf. Rev.* **2014**, *1*, 20. [CrossRef]
25. Liu, Y.; Liu, H.D.; Pelenovich, V.; Wan, Q.; Guo, J.L.; Chen, Y.M.; Zhang, J.; Xue, L.J.; Li, Z.G.; Yang, B. Influences of modulation period on structure and properties of AlTiSiN/AlCrSiN nanocomposite multilayer coatings. *Vacuum* **2021**, *193*, 110516. [CrossRef]
26. Esposito, A.M.; He, Q.; DePaiva, J.M.; Veldhuis, S.C. Significance of tool coating properties and compacted graphite iron microstructure for tool selection in extreme machining. *Nanomaterials* **2025**, *15*, 130. [CrossRef] [PubMed]
27. Lai, D.; Huang, R.; Li, S.; Zhang, J.; Deng, Q.; Deng, T.; Liao, X.; Lin, Y. Microscopic numerical simulation and experimental investigation on the machining process of compacted graphite cast iron (CGI) considering microstructure and different tool wear states. *Int. J. Precis. Eng. Manuf.* **2026**, *27*, 2445–2463. [CrossRef]
28. Liu, Z.Q.; Ai, X. High-speed milling of cast iron with ceramic and PCBN tools. *Key Eng. Mater.* **2004**, *259–260*, 446–450. [CrossRef]
29. Schultheiss, F.; Bushlya, V.M.; Lenrick, F.; Johansson, D.; Kristiansson, S.; Ståhl, J.-E. Tool wear mechanisms of pcBN tooling during high-speed machining of gray cast iron. *Procedia CIRP* **2018**, *77*, 606–609. [CrossRef]
30. Mia, M.; Rahman, M.A.; Gupta, M.K.; Sharma, N.; Danish, M.; Prakash, C. Advanced cooling-lubrication technologies in metal machining. In *Machining and Tribology, Processes, Surfaces, Coolants, and Modeling*, 1st ed.; Pramanik, A., Ed.; Elsevier: Amsterdam, The Netherlands, 2021; pp. 67–92.
31. Mardonov, U.; Khasanov, O.; Yang, Y.; Yatskevich, O.; Akramov, M.; Abdullaev, B. Studying the effect of diverse lubricating and cooling environments in turning gray cast iron. *Int. J. Mechatron. Appl. Mech.* **2025**, *22*, 213–223.
32. Peixoto, A.C.S.; Fernandes, G.H.N.; Martins, P.S.; Barbosa, L.M.Q.; França, P.H.P.; da Silva, M.B.; Costa, É.S.; Baldin, V.; da Silva, W.M., Jr.; Machado, Á.R. Machining gray cast iron with internally cooled tools: Performance, wear, and sustainability assessment. *Int. J. Adv. Manuf. Technol.* **2025**, *138*, 2605–2626. [CrossRef]
33. Fernandes, G.H.N.; Bazon, V.T.; Barbosa, L.M.Q.; França, P.H.P.; da Silva, M.B.; Uddin, M.; Martins, P.S.; Machado, Á.R. Performance comparison between internally cooled tools and flood cooling during grey cast iron turning. *J. Manuf. Process.* **2023**, *85*, 817–831. [CrossRef]
34. Cakir, M.C.; Isik, Y. Investigating the machinability of austempered ductile irons having different austempering temperatures and times. *Mater. Des.* **2008**, *29*, 937–942. [CrossRef]
35. Sharun, V.; Anand Ronald, B. Traditional machining of austempered ductile iron (ADI): A review. *Mater. Today Proc.* **2023**, *72*, 2027–2031. [CrossRef]
36. Shankar, S.; Mohanraj, T.; Thangarasu, S.K. Multi-response milling process optimization using the Taguchi method coupled to grey relational analysis. *Mater. Test.* **2016**, *58*, 462–470. [CrossRef]
37. Mastan Rao, P.; Deva Raj, C.; Dhoria, S.H.; Vijaya, M.; Ranga Raya Chowdary, J. Multi-objective optimization of turning for nickel-based alloys using Taguchi-GRA and TOPSIS approaches. *J. Inst. Eng. India Ser. D* **2024**, *105*, 1473–1484.
38. Yigit, R.; Celik, E.; Findik, F.; Koksal, S. Effect of cutting speed on the performance of coated and uncoated cutting tools in turning nodular cast iron. *J. Mater. Process. Technol.* **2008**, *204*, 80–88. [CrossRef]
39. Nayyar, V.; Kaminski, J.; Kinnander, A.; Nyborg, L. An experimental investigation of machinability of graphitic cast iron grades; flake, compacted and spheroidal graphite iron in continuous machining operations. *Procedia CIRP* **2012**, *1*, 488–493. [CrossRef]
40. Gasmi, B.; Yallese, M.A.; Boucherit, S.; Chihaoui, S.; Mabrouki, T. Experimental investigation on the performance of ceramics and CBN cutting materials during dry machining of cast iron: Modeling and optimization study using RSM, ANN, and GA. *Proc. Inst. Mech. Eng. Part C J. Mech. Eng. Sci.* **2024**, *238*, 1397–1422.
41. Ma, H.-L.; Sun, B.-J.; Zhang, J.-H. Wear behaviors of PcBN milling insert in high-speed dry milling nodular cast iron. *J. Braz. Soc. Mech. Sci. Eng.* **2024**, *46*, 521. [CrossRef]
42. European Steel and Alloy Grades/Numbers. Available online: https://www.steelnumber.com/en/steel_composition_eu.php?name_id=1536#1 (accessed on 19 June 2026).
43. Varela-Fernández, N. Mechanical Behaviour and Marine Corrosion of Various Ferrous Alloys Used in Ships and Their Components. Ph.D. Thesis, University of A Coruña, A Coruña, Spain, 2016. (In Spanish)
44. *PN-EN 1563*; Founding, Spheroidal Graphite Cast Irons. Polish Committee for Standardization: Warsaw, Poland, 2018.
45. Zych, J.S. *Spheroidal Graphite Cast Iron: Feeding Castings, Pouring Moulds*; Akapit Academic Publishing House: Cracow, Poland, 2019. (In Polish)
46. Rhenus TS 223 T. Available online: https://www.rhenuslub.de/en/produkt/rhenus-ts-223-t/ (accessed on 10 July 2026).
47. Tungaloy, Milling, General Catalog—Vol. 2. Available online: https://tungaloy.com/pl/pdf/?file=https://tungaloy.com/wpdata/wp-content/uploads/GC_2023-2024_G_Milling.pdf#zoom=page-fit&pagemode=none (accessed on 19 June 2026).
48. de Souza Silva, D.; da Costa, A.F. Chips generated during the machining of SAE-8620 using carbide inserts coated with (TiAl)N by the PVD process. *Biol. Chem. Res.* **2020**, *7*, 139–153.
49. New CVD Coated Grade for Milling Cast Iron, T1115. Available online: https://tungaloy.com/wpdata/wp-content/uploads/395-u_T1115.pdf (accessed on 10 July 2026).

50. New PVD Coated Grade for Milling, AH130. Available online: https://tungaloy.com/wpdata/wp-content/uploads/383.pdf (accessed on 10 July 2026).
51. Skiba, J.; Kulczyk, M.; Przybysz-Gloc, S.; Skorupska, M.; Kobus, M.; Nowak, K. Industrial-scale copper wear reduction in the electrical discharge machining through hydrostatic extrusion. *Materials* **2026**, *19*, 1314. [CrossRef] [PubMed]
52. Sługocka, M.; Grochała, D.; Kwiatkowski, K.; Grzejda, R.; Zmarzły, P. Study of the impact of surface topography on selected mechanical properties of adhesive joints. *Coatings* **2024**, *14*, 944. [CrossRef]
53. Grochała, D.; Jasiewicz, M.; Filipowicz, K.; Parus, A.; Powałka, B.; Grzejda, R.; Zmarzły, P. Assessment of the functional properties of the surfaces of ductile cast iron parts. *Appl. Sci.* **2024**, *14*, 9129. [CrossRef]
54. *PN-EN ISO 4288*; Geometrical Product Specifications (GPS), Surface Texture: Profile Method, Rules and Procedures for the Assessment of Surface Texture. Polish Committee for Standardization: Warsaw, Poland, 2011.
55. Grochala, D.; Bachtiak-Radka, E.; Dudzińska, S. The investigations of the surface characteristics by methods of the optical scanning—Requirements and measurements according with the guidelines of the PN-EN ISO 25178. *Weld. Technol. Rev.* **2016**, *88*, 92–96. [CrossRef]
56. Żyłka, W.M.; Świrk, P.; Pater, M.A.; Leniowska, L. Influence of paint coatings on the sound absorption coefficient. *Adv. Sci. Technol. Res. J.* **2026**, *20*, 130–142. [CrossRef]
57. *PN-ISO 3685*; Tool-Life Testing with Single-Point Turning Tools. Polish Committee for Standardization: Warsaw, Poland, 1996.
58. Grudzień, J.; Grochała, D.; Grzejda, R.; Kochmański, P. Testing the effectiveness of hybrid milling and surface burnishing in improving the wear resistance of machine parts made of structural steel. *Lubricants* **2024**, *12*, 458. [CrossRef]
59. Ochal, A.; Grochała, D.; Grzejda, R.; Kochmańska, A.E. Investigations on changes in the surface geometrical texture caused by the use of corrosion product removers. *Coatings* **2025**, *15*, 539. [CrossRef]
60. Kwon, Y.; Fischer, G.W. A novel approach to quantifying tool wear and tool life measurements for optimal tool management. *Int. J. Mach. Tools Manuf.* **2003**, *43*, 359–368. [CrossRef]
61. Yu, Z.; Zheng, Y.; Sun, J.; Zhao, J. Recent advances in toughening of alumina-based ceramic machining tools. *Int. J. Refract. Met. Hard Mater.* **2026**, *134*, 107436. [CrossRef]
62. Kobayashi, F.; Okuno, S.; Ichikawa, T.; Tanaka, K.; Imamura, S. New milling grades—ACU2500 for general purposes, ACP2000/ACP3000 for steel milling, and ACK2000/ACK3000 for cast iron milling. *SEI Tech. Rev.* **2020**, *90*, 81–85.